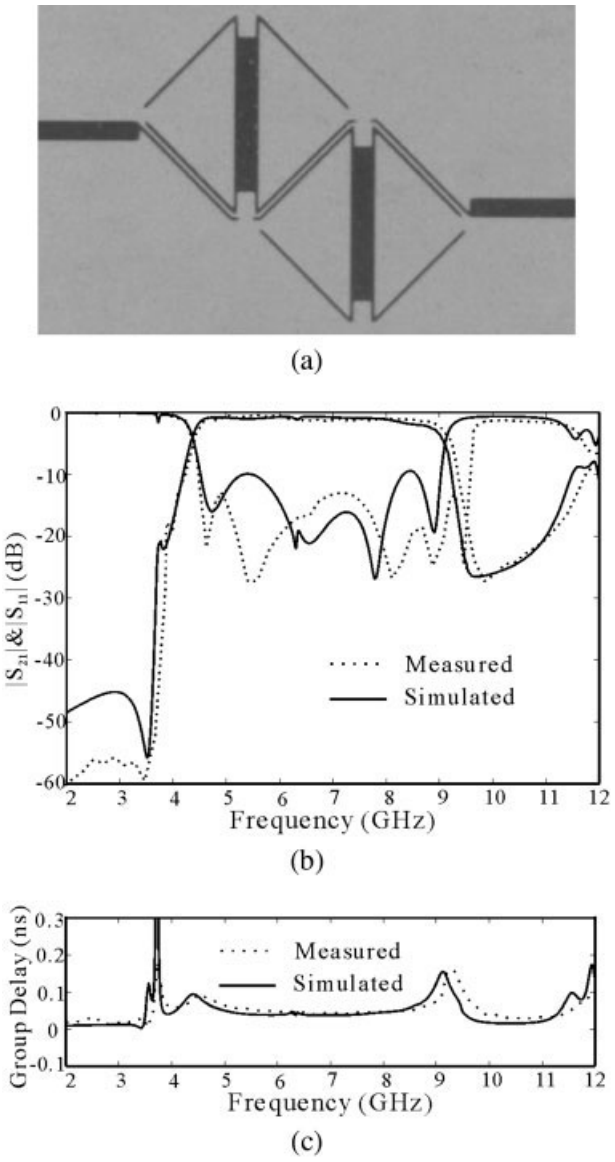

Figure 4 Predicted and measured results of the proposed double-stage triple-mode wideband bandpass filter. (a) Photograph. (b) S_{11}- and S_{21}-magnitudes. (c) Group delay

with measured insertion loss 1.3 dB and group delay around 0.52 ns at the center frequency of the passband. The 3-dB passband is slightly narrowed to the band of 4.3 to 9.2 GHz due to highly sharpened rejection skirt in the lower and upper cut-off frequencies of this two-stage wideband filter.

4. CONCLUSION

A rhombus-shaped triple-mode MMR has been proposed and characterized in this work to build up a class of compact wideband bandpass filters with sharpened rejection skirts. In this modified MMR, a two-section open-circuited stub is attached to the center of a uniform half-wavelength resonator. By properly raising the ratio of characteristic impedances or strip widths in these two sections, a TMR with intrinsic transmission zeros below and above the desired passband can be build up. Using this MMR together with parallel coupled lines, two wideband bandpass filters with single and double rhombus-shaped TMRs are designed and fabricated. Both predicted and measured results have not only exhibited good wide passband with low insertion loss and small group delay but also exposed highly rejection skirt in both lower and higher upper cut-off frequencies.

REFERENCES

1. L. Zhu, S. Sun, and W. Menzel, Ultra-wideband (UWB) bandpass filters using multiple-mode resonator, IEEE Microwave Wireless Compon Lett 15 (2005), 796–798.
2. S.W. Wong and L. Zhu, EBG-embedded multiple-mode resonator for UWB bandpass filter with improved upper-stopband performance, IEEE Microwave Wireless Compon Lett 17 (2007), 421–423.
3. J.-R. Lee, J.-H. Cho, and S.-W. Yun, New compact bandpass filter using microstrip/4 resonators with open stub inverter, IEEE Microwave Wireless Compon Lett 10 (2000), 526–527.
4. L. Zhu and W. Menzel, Compact microstrip bandpass filter with two transmission zeros using a stub-tapped half-wavelength line resonator, IEEE Microwave Wireless Compon Lett 13 (2003), 16–18.
5. C. Quendo, E. Rus, C. Person, J.-F. Favennec, Y. Clavet, A. Manchec, R. Bairavasubramanian, S. Pinel, J. Papapolymerou, and J. Laskar, Wide band, high rejection and miniaturized fifth order banpass filter on LCP low cost organic substrate, IEEE MTT-S Int Dig, Long Beach, CA (2005), 2203–2205.
6. K.M. Shum, W.T. Luk, C.H. Chan, and Q. Xue, A UWB bandpass filter with two transmission zeros using a single stub with CMRC, IEEE Microwave Wireless Compon Lett 17 (2007) 43–45.

HARMONIC SUPPRESSED AND SIZE-REDUCED BANDSTOP AND BANDPASS FILTERS

Majeed A. S. Alkanhal and Ashraf S. Mohra
Department of Electrical Engineering, King Saud University, Riyadh, Saudia Arabia; Corresponding author: ashraf_mohra@yahoo.com

Received 23 November 2008

ABSTRACT: *New bandstop/bandpass microstrip structures with harmonic suppression are presented in this article. By replacing the series quarter-wavelength connecting lines of conventional open-stub bandpass/bandstop filters with the equivalent* Π*-shaped line section, compact open-stub bandstop/bandpass filters with second harmonic suppression are achieved. Transmission-line theory is used to derive the design equations of the equivalent* Π*-shaped lines. Simulation and experiments have also been done to validate the proposed design concept. When compared with the conventional open-stub Bandpass/Bandstop filters, the second harmonic is suppressed and size reduction is achieved in both the Bandstop/bandpass structures. Moreover, results confirm that the proposed shaped bandpass filter achieves a further third harmonic rejection.* © 2009 Wiley Periodicals, Inc. Microwave Opt Technol Lett 51: 2109–2114, 2009; Published online in Wiley InterScience (www.interscience.wiley.com). DOI 10.1002/mop.24580

Key words: *bandpass filter; bandstop filter; compact filters; harmonic suppression*

1. INTRODUCTION

Bandstop and bandpass filters (BSFs and BPFs) are key building blocks in modern microwave communication systems. Such filters play the main role of filtering out the unwanted signals and passing the desired signals. Conventional filters that consist of transmission lines or uniform distributed elements encounter a problem on the passband region imposed by the periodicity of the distributed elements. This causes the stopbands to repeat at odd multiples of

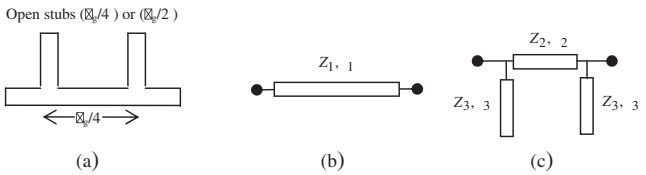

Figure 1 (a) Conventional bandstop or bandpass filter (b) Original connecting transmission line (c) The equivalent Π-shaped section

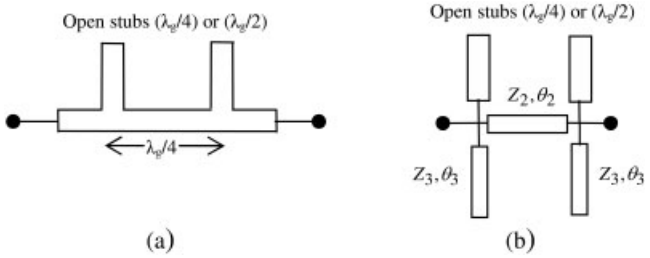

Figure 3 The schematic of the bandstop/bandpass filter, (a) the conventional filter and (b) the modified filter

the fundamental stopband center frequency and the passpands to repeat at even multiples of the fundamental passband frequency.

Several conventional structures of bandpass/bandstop filters like end-coupled filters, parallel-coupled filters, and open-stub filters could meet the specification at the fundamental frequency band. However, due to the distributed characteristics of the transmission lines, these filters suffer from the problem of spurious passbands. Numerous efforts have been contributed to enhance and control the size, the rejection bandwidth and the passbands of the microstrip filters. Insertion of an additional bandstop filter is the most straightforward method to suppress the harmonics [1, 2]. However, this would also increase the insertion loss in the passband and the overall filter size. Many useful methods have shown promising results dealing with the harmonic problems. Stepped-impedance resonator filters, controlled input and output tapping filters, stub-tapped line resonator filters, and the electromagnetic-bandgap (EBG)-based filters have been used to enhance the second passband [3–6]. Shaped configurations such as wiggly and corrugated line filters have a second harmonic suppression improvement over 30 dB [7, 8]. Integration of low-pass filters in a bandpass filter and in dual behavior resonator (DBR) filters for out-of-band improvement is described in [9, 10]. In [11], a quarter-wavelength shunt open stub is added to a fixed half-wavelength resonator to introduce an attenuation pole and work as an inverter. A spurline has been used to improve the stopband rejection for a bandstop filter [12]. A technique that presents a noticeable second harmonic suppression through integration of bandstop filters with the bandstop or bandpass filters using T-shaped line sections is presented in [13].

In this article, new configurations for harmonic suppression of the conventional bandstop or bandpass filter are described. These configurations are based on replacing the series connecting lines of the conventional open-stub bandstop and bandpass filters with equivalent Π-shaped lines. The proposed filters have compact sizes beside their perfect second harmonic suppression. General design equations for generating the parameters of the equivalent Π-shaped lines are derived using transmission-line theory. The equivalent Π-shaped lines show good similarities with the original line around the specific fundamental passband. Hence, the passband/stopband response of the proposed filters is the same as the conventional ones. Furthermore, the Π-shaped section integrates a bandstop filter at the second harmonic. Therefore, the proposed filters have a second harmonic rejection advantage over the conventional ones. The concept of the proposed filters is validated by full-wave electromagnetic (EM) simulations. Further numerical modeling, experimentation and geometrical shaping to optimize the proposed filters in terms of performance and space efficiency are carried out for both filter types. In addition, both of the attained compact size filters have been realized on RT/Duroid ($\varepsilon_r = 2.2$, $h = 1.5748$ mm), and their measurements are ascertained to have a superior second harmonic suppression. Simulation and measurements demonstrate that the proposed shaped BPF achieves a remarkable further third harmonic rejection too.

2. EQUIVALENT Π-SHAPED TRANSMISSION LINES

Figure 1(a) shows the conventional bandstop/bandpass filter with open-stub sections separated by quarter-wavelength connecting transmission lines. A transmission line section, and its equivalent Π-shaped transmission-line model are shown in Figures 1(b) and (c), respectively, where Z_i is the characteristic impedance, Y_i is the characteristic admittance, and θ_i is the electrical length of the transmission lines ($i = 1, 2, 3$). The series quarter-wavelength connecting line ($\lambda_g/4$ section) of the conventional bandpass/bandstop filter of Figure 1(a) is converted to a Π-shaped transmission line section. The Π-shaped transmission-line model of Figure 1(c) is consisted of two identical shunt open stub transmission lines and one series element connecting the two shunt stubs. To study how the Π-shaped transmission line section can be equivalent to the original transmission line, transmission-line model calculation is

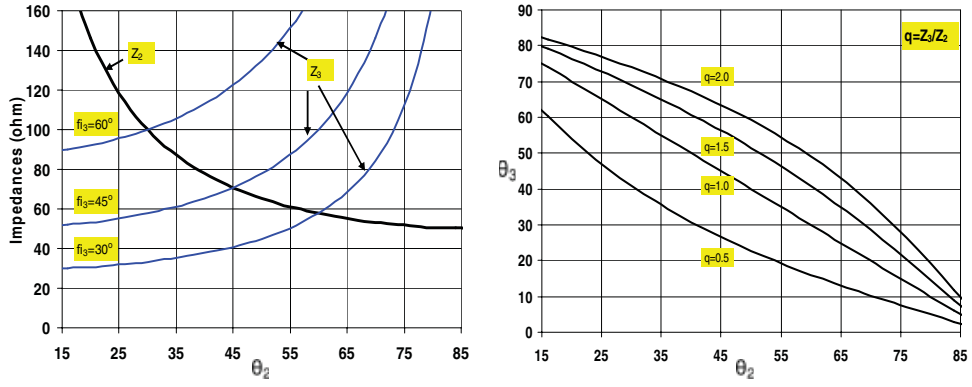

Figure 2 The variations of Z_1, Z_2, and θ_3 versus θ_2. [Color figure can be viewed in the online issue, which is available at www.interscience.wiley.com]

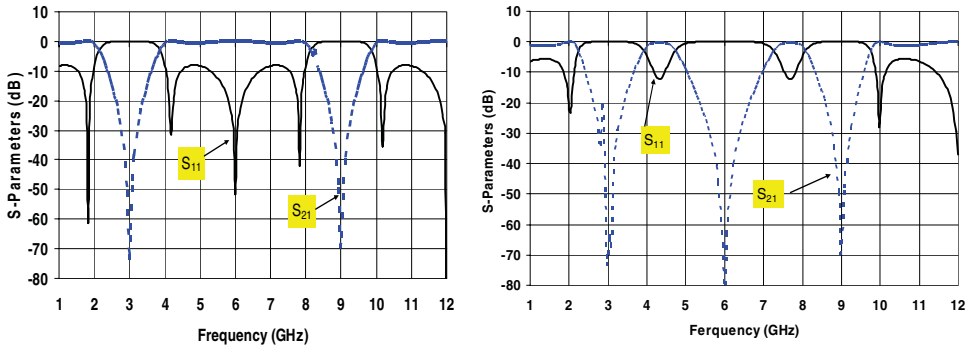

Figure 4 TL simulation results of the conventional and the modified bandpass filters, (a) the simulated S-parameters for conventional bandstop filter and (b) the simulated S-parameters for modified bandstop filter before optimization. [Color figure can be viewed in the online issue, which is available at www.interscience.wiley.com]

used. The conversion of the transmission line to its Π-shaped line is based on the ABCD parameter matrices of both sections.

The ABCD matrix for the original transmission line of Figure 1(b), with electrical length ($\theta_1 = \lambda_g/4$) is given by:

$$M_1 = \begin{bmatrix} 0 & jZ_1 \\ jY_1 & 0 \end{bmatrix} \tag{1}$$

The ABCD matrix for the Π-shaped transmission line section of Figure 1(c) is

$$M_T = M_3 M_2 M_3 \tag{2}$$

where M_2 is the ABCD matrix for the series element and is given by

$$M_2 = \begin{bmatrix} \cos\theta_2 & jZ_2 \sin\theta_2 \\ jY_2 \sin\theta_2 & \cos\theta_2 \end{bmatrix}, \tag{3}$$

and M_3 is the ABCD matrix for each of the shunt opens stubs elements and is given by

$$M_3 = \begin{bmatrix} 1 & 0 \\ jY_3 \tan\theta_3 & 1 \end{bmatrix} \tag{4}$$

Equating the individual elements of the ABCD matrices of Eqs. (1) and (2), the impedances of the equivalent Π-shaped section will be as follows:

$$Z_2 = Z_1/\sin(\theta_2) \tag{5}$$

$$Z_3 = Z_2 \cdot \tan((\theta_2) \cdot \tan(\theta_3) \tag{6}$$

For compact size, the electrical length θ_2 must be less than $\pi/2$, while, for practical microstrip realization, the impedance must be bounded in the region ($160\ \Omega < Z < 30\ \Omega$). Figure 2 illustrates the variations of each of the series impedance (Z_2) against θ_2, and the variation of (Z_3) at different values of θ_3 against θ_2. For compact θ_2 size, the value of θ_3 must be large and vice versa, so θ_2 value must be carefully selected to achieve all requirements of impedance realization and size compactenss.

3. DESIGN OF BANDSTOP FILTERS WITH SECOND HARMONIC SUPPRESSION

The conventional bandstop filter is shown in Figure 3(a), with two open stubs and a connecting series section, all with length of $\lambda_g/4$. The modified bandstop filter is shown in Figure 3(b), where the series section is replaced by its equivalent Π-section. Choosing $\theta_2 = \theta_3 = \pi/4$, the values of the characteristic impedances based on Eqs. (5) and (6) will be $Z_2 = Z_3 = 70.71\ \Omega$. The conventional and the modified bandstop filters are designed at 3 GHz on, RT/Duroid

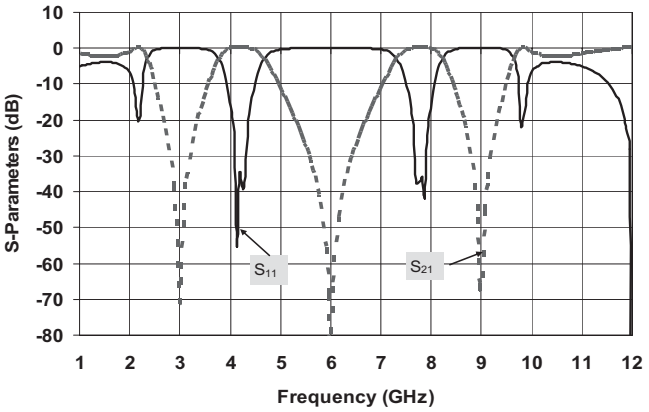

Figure 5 TL simulated S-parameters for the (optimized) modified bandstop filter

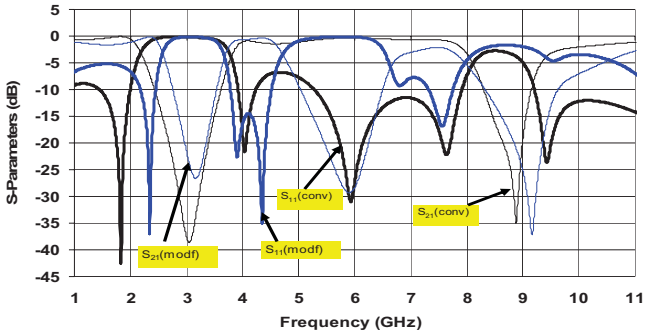

Figure 6 The full-wave EM simulation results for the conventional (conv) and the (optimized) modified (modf) bandstop filters. [Color figure can be viewed in the online issue, which is available at www.interscience.wiley.com]

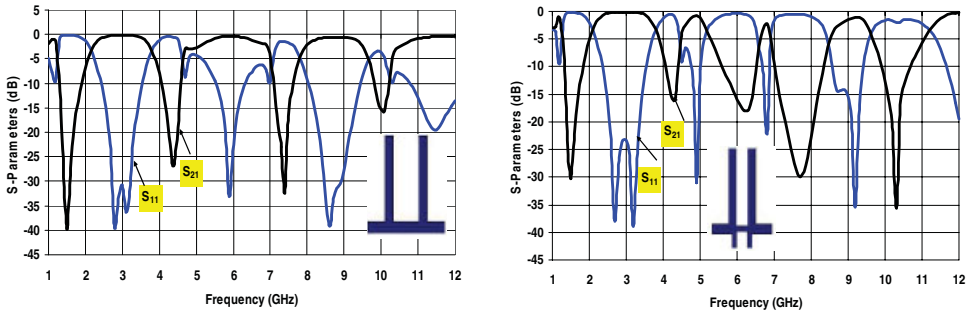

Figure 7 The full-wave EM-simulated scattering parameters, (a) conventional filter and (b) modified bandpass filter. [Color figure can be viewed in the online issue, which is available at www.interscience.wiley.com]

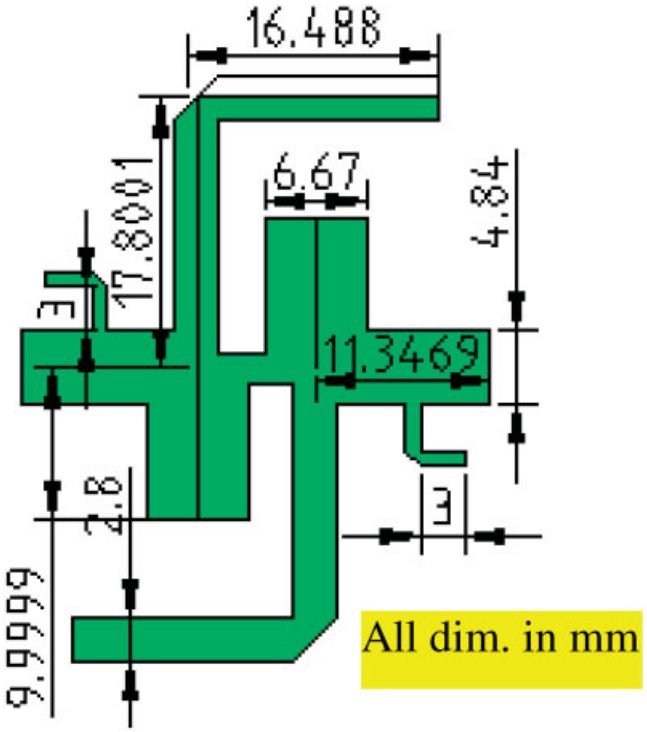

Figure 8 The dimensions for the shaped (optimized) modified bandpass filter. [Color figure can be viewed in the online issue, which is available at www.interscience.wiley.com]

($\varepsilon_r = 2.2$, $h = 1.5748$ mm), and then simulated using transmission line (TL)-based software. The simulation results for both types are shown in Figure 4. There is obvious added suppression of the second harmonics at 6 GHz in the modified bandstop filter similar to that suppression obtained using T-line transformation [13, 14]. Simple optimization was done for the series impedance (Z_2) to enhance the design. The new optimized value was found to be 55 Ω. The simulation results for the (optimized) modified bandstop fitter are shown in Figure 5.

For more practical investigation of the BSF configurations, a full wave electromagnetic (EM) simulation is carried out for the conventional and the optimized modified bandstop filters. The results are shown in Figure 6. For the conventional bandstop filter, there are two transmission zeros at 3 and 9 GHz, and a passband located at the second harmonic frequency of 6 GHz. The (optimized) modified bandstop filter has zeros at 3, 6, and 9 GHz. With its compact size, this bandstop filter can be efficiently used as a dc-pass output filter. The dc-pass filter is required to have suppression in harmonics, as well as the fundamental frequency. If this dc-pass filter is used in a rectenna system, the efficiency of the rectenna will increase because more energy is reflected by the output filter and remixes within the diode to generate higher dc output [14].

4. DESIGN OF BANDPASS FILTERS WITH SECOND HARMONIC SUPPRESSION

The conventional bandpass filter is shown in Figure 3(a), where the electrical length is $\lambda_g/4$ for the series section, and $\lambda_g/2$ for the open

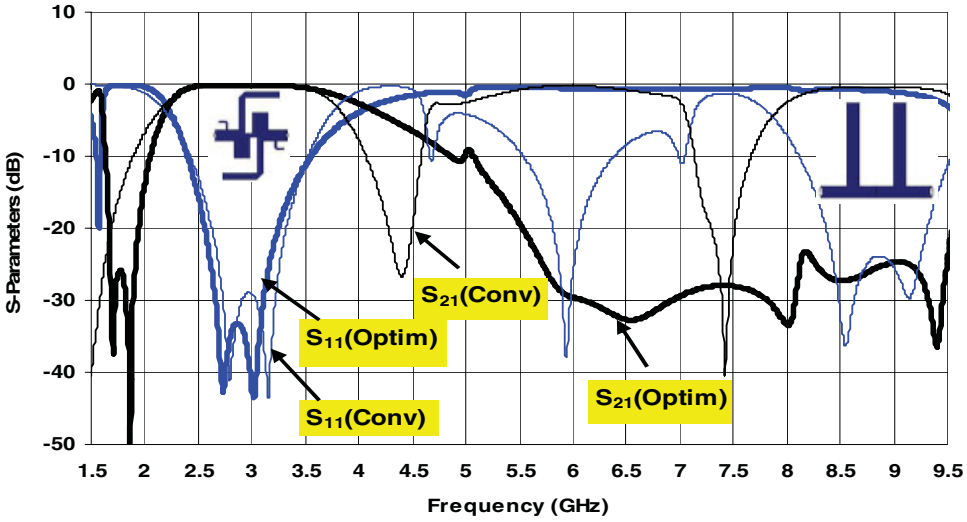

Figure 9 The full-wave simulated S-parameters for the conventional and the shaped bandpass filters. [Color figure can be viewed in the online issue, which is available at www.interscience.wiley.com]

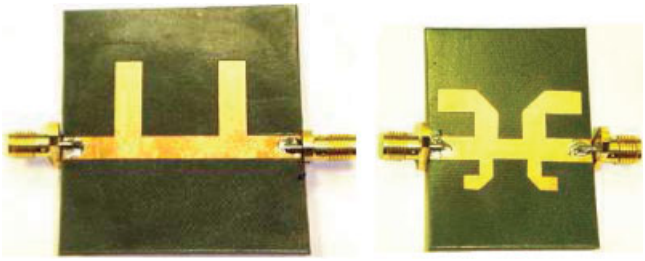

Figure 10 The photo of the realized band stop filters. [Color figure can be viewed in the online issue, which is available at www.interscience.wiley.com]

stubs (or $\lambda_g/4$ for shorted stubs). The modified bandpass filter is done by replacing the series section by its equivalent π-section with the same values that used with the modified bandstop filter case ($\theta_2 = \theta_3 = \pi/4$, $Z_2 = Z_3 = 70.71\ \Omega$). The conventional and the modified bandpass filters are designed at 3 GHz on RT/Duroid ($\varepsilon_r = 2.2$, $h = 1.5748$ mm), and then simulated using a full-wave EM software. The simulated results are shown in Figure 7. The conventional bandpass filter have a passbands at 3, 6, and 9 GHz, while the modified bandpass filter have a passband at 3 GHz and a stopband (suppressed passband) at 6 GHz. The modified bandpass filter in its basic form suffers from two mild passband notches at 4.9 and 6.8 GHz. Optimization and shaping are used on the impedances and lengths of each of the Π-section and the open stubs to further, effectively, suppress the third passband at 9 GHz of the modified bandpass filter and make the filter more space efficient too. Also by adding two stubs at the input terminals of the filters, the parasitic mild passbands at 4.9 and 6.8 GHz are suppressed. The dimensions of the reduced-size shaped (optimized)-modified bandpass filter are shown in Figure 8. The simulated results for the conventional and the shaped bandpass filters are shown in Figure 9.

5. REALIZATION AND MEASUREMENTS OF THE BANDSTOP AND BANDPASS FILTERS

Both the conventional and the (optimized0 modified bandstop filters are realized on RT/Duroid ($\varepsilon_r = 2.2$, $h = 1.5748$ mm) at 3 GHz using thin-film and photolithographic techniques. Figure 10 illustrates the photo of the realized bandstop filters. The comparisons between the simulated and measured results for the (optimized) modified bandstop filter are illustrated in Figure 11. The simulated and measured results are in a very good agreement and the realized (optimized) modified bandstop filter achieves zeros at 3, 6, and 9 GHz with values of −21, −28, and −18 dB, respectively, with an evident second harmonic suppression.

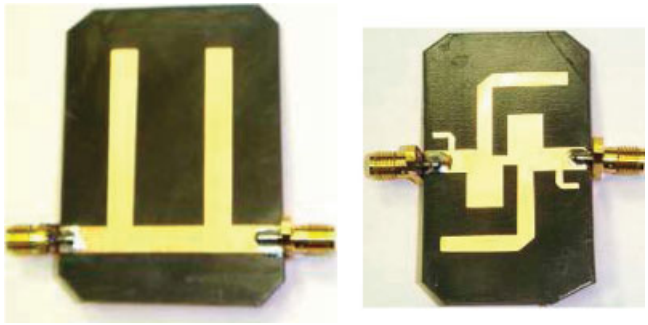

Figure 12 The photo of the realized band pass filters. [Color figure can be viewed in the online issue, which is available at www.interscience.wiley.com]

Both the conventional and the (shaped) modified bandpass filters are realized on the same material and at same frequency as the case of the bandstop filters. Figure 12 illustrates the photo of the realized bandpass filters. The measured results for the shaped modified bandpass filter are illustrated in Figure 13. The measured results demonstrate the suppression of the passbands at 6 and 9 GHz for the proposed filter configuration.

6. CONCLUSIONS

A technique that accomplishes a significant second harmonic suppression through integration of bandstop filter with bandstop or bandpass filters using Π-shaped sections is presented. Without affecting the fundamental frequency response, the proposed filters show superior second harmonic suppression in addition to their compact sizes. Further performance optimization and geometry shaping of the proposed filters have been carried out using full-wave electromagnetic simulations. Excessively, the presented shaped BPF achieves a further

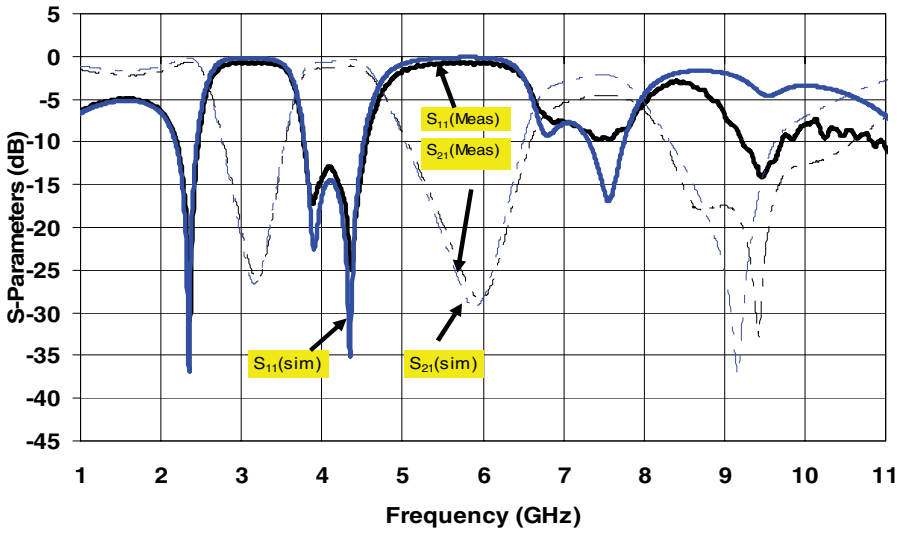

Figure 11 Simulated and measured S-parameters for the (optimized) modified bandstop filter. [Color figure can be viewed in the online issue, which is available at www.interscience.wiley.com]

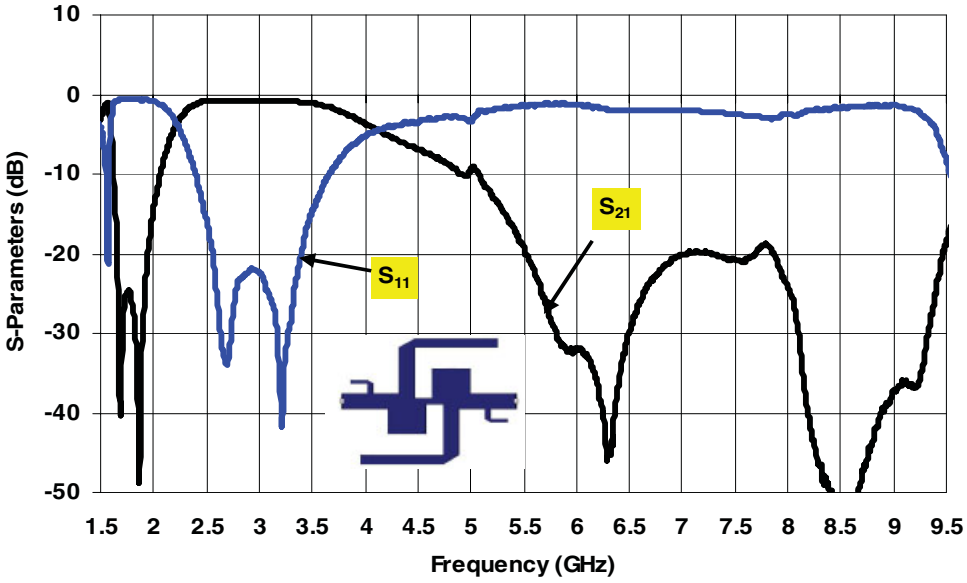

Figure 13 The measured S-parameters of the shaped bandpass filter. [Color figure can be viewed in the online issue, which is available at www.interscience.wiley.com]

prominent third harmonic rejection. The proposed filters have been realized and validated experimentally.

ACKNOWLEDGMENTS

The authors of this article would like to acknowledge the assistance and the financial support provided by the Research Center in the College of Engineering at King Saud University.

REFERENCES

1. L.-H. Hsieh and K. Chang, Piezoelectric transducer tuned bandstop filter, Electron Lett 38 (2002), 970–971.
2. J. Garcia-Garcia, F. Martin, F. Falcone, J. Bonache, I. Gil, T. Lopetegi, M.A.G. Laso, M. Sorolla, and R. Marques, Spurious passband suppression in microstrip coupled line bandpass filters by means of split ring resonators, IEEE Microwave Wireless Compon Lett 14 (2004), 416–418.
3. M. Makimoto and S. Yamashita, Bandpass filters using parallel coupled stripline stepped impedance resonators, IEEE Trans Microwave Theory Tech 28 (1980), 1413–1417.
4. J.-T. Kuo and E. Shih, Microstrip stepped impedance resonator bandpass filter with an extended optimal rejection bandwidth, IEEE Trans Microwave Theory Tech 51 (2003), 1554–1559.
5. Y.W. Kong and S.T. Chew, EBG-based dual mode resonator filter, IEEE Microwave Wireless Compon Lett 14 (2004), 124–126.
6. L. Zhu and W. Menzel, Compact microstrip bandpass filter with two transmission zeros using a stub-tapped half-wavelength line resonator, IEEE Microwave Wireless Compon Lett 13 (2003), 16–18.
7. J.-T. Kuo, W.-H. Hsu, and W.T. Huang, Parallel coupled microstrip filters with suppression of harmonic response, IEEE MicrowaveWireless Compon Lett 12 (2002), 383–385.
8. T. Lopetegi, M.A.G. Laso, J. Hernandez, M. Bacaicoa, D. Benito, M.J. Garde, M. Sorolla, and M. Guglielmi, New microstrip 'wiggly line' filters with spurious passband suppression, IEEE Trans Microwave Theory Tech 49 (2001), 1593–1598.
9. C. Quendo, E. Rius, C. Person, and M. Ney, Integration of optimized low-pass filters in a bandpass filter for out-of-band improvement, IEEE Trans Microwave Theory Tech 49 (2001), 2376–2383.
10. A. Manchec, C. Quendo, E. Rius, C. Person, and J.-F. Favennec, Synthesis of dual behavior resonator (DBR) filters with integrated low-pass structures for spurious responses suppression, IEEE Microwave Wireless Compon Lett 16 (2006), 4–6.
11. J.-R. Lee, J.-H. Cho, and S.-W. Yun, New compact bandpass filter using microstrip λ/4 resonators with open stub inverter, IEEE Microwave Guided Wave Lett 10 (2000), 526–527.
12. W.-H. Tu and K. Chang, Compact microstrip bandstop filter using open stub and spurline, IEEE Microwave Wireless Compon Lett 15 (2005), 268–270.
13. W.-H. Tu and K. Chang, Compact second harmonic-suppressed bandstop and bandpass filters using open stubs, IEEE Microwave Theory Tech 54 (2006), 2479–2502.
14. Y.-H. Suh, C. Wang, and K. Chang, Circularly polarized truncated corner square patch microstrip rectenna for wireless power transmission, Electron Lett 36 (2000), 600–602.

BANDWIDTH ENHANCEMENT OF A QUARTER-WAVELENGTH SLOT ANTENNA BY CAPACITIVE LOADING

Zidong Liu and Kevin Boyle
NXP Semiconductors, Cross Oak Lane, Redhill, Surrey RH1 5HA, United Kingdom; Corresponding author: zidong.liu@ntlworld.com

Received 23 November 2008

ABSTRACT: *In this article, a novel wideband slot antenna is proposed. The slot is quarter-wavelength long and loaded with a capacitor to increase its bandwidth. The effect of the capacitor on the antenna radiation efficiency is also investigated.* © 2009 Wiley Periodicals, Inc. Microwave Opt Technol Lett 51: 2114–2116, 2009; Published online in Wiley InterScience (www.interscience.wiley.com). DOI 10.1002/mop.24579

Key words: *slot; antenna; mobile phone*

1. INTRODUCTION

The dual-band inverted-F antenna is widely used in mobile phones to cover the cellular frequency bands due to its desirable features of compactness, high efficiency, and low SAR [1, 2]. However, it is likely that in future an additional handset antenna will be required to operate between 2 and 6 GHz for WiFi/WiMAX,